

汽车用镁/钢异种金属冷金属过渡点焊工艺特性

许庆伟¹, 曹 睿¹, 陈剑虹¹, 王培中²

(1. 兰州理工大学 省部共建有色金属先进加工与再利用国家重点实验室, 兰州 730050;

2. 通用汽车公司 北美研发中心, 美国 沃伦 48090)

摘 要: 采用冷金属过渡的方法对 AZ31B 变形镁合金和镀锌钢板进行搭接点焊试验, 运用正交试验法优化工艺参数, 同时利用光学显微镜、扫描电镜和万能拉伸试验机对焊接接头的微观组织和力学性能进行研究。结果表明, 运用冷金属过渡方法能够获得成形美观和性能良好的焊接接头; 工艺参数显著性顺序为镀锌钢板孔径大小、送丝速度、点焊时间; 接头为典型的点熔钎焊接头, 由钎焊结合区和熔焊结合区组成; 接头的抗拉剪载荷可达 3.12 kN, 远大于相同尺寸下镁镁点焊试样的抗拉剪载荷, 接头的断裂方式为剪切型断裂和撕裂型断裂。

关键词: 冷金属过渡点焊; 异种金属; 工艺特性; 正交试验

中图分类号: TG 457.19 **文献标识码:** A **文章编号:** 0253-360X(2014)05-0043-04

0 序 言

近年来随着能源危机和环境问题的日益严重, 节能减排成为当前汽车工业的重要课题。面对这一压力, 在优化电子燃油喷射系统、降低风阻系数、轻量化制造材料等应对措施中, 最直接有效的还是后者, 即在占整车自重分别为 28% 和 27% 的车身和底盘中大量采用轻量化材料技术。

镁合金是目前可应用的最轻的结构材料, 因而成为汽车减轻自重以提高其节能性和环保性的首选材料。另外镁合金材料还具有比强度和比刚度高、易加工成形、废料易回收等特点^[1-2]。所以在汽车工业中, 镁和钢异种金属焊接结构的应用将越来越广泛, 实现镁和钢连接将具有十分重要的意义。

镁和钢的熔点以及热物理性能相差很远, 同时镁和钢之间没有固溶度, 既不能形成固溶体也不能形成金属间化合物, 所以这些因素给镁钢的连接造成了极大的困扰^[3-4]。尽管扩散焊^[5]、搅拌摩擦焊^[6-7]、镍夹层激光电弧复合焊^[8-9]、激光熔钎焊^[10, 11]等方法可以实现镁/钢异种金属的连接, 但这些方法易受工件形状和尺寸的限制, 成本高昂, 焊接过程复杂等因素难以满足大批量生产的需求。

冷金属过渡技术作为一种新型的焊接方法, 具有焊接质量好、热输入低、无飞溅起弧、焊接变形小等特点, 特别适合用于自动焊, 尤其适合用于异种金

属的连接。由于在汽车工业中点连接应用最为广泛, 并且冷金属过渡点焊工艺变形更小, 所以文中采用冷金属过渡点焊的方法来实现汽车用镁钢异种金属的连接, 并通过正交试验法获得最佳工艺参数, 同时根据接头的力学性能和微观组织确定冷金属过渡点焊的工艺特性, 为以后的深入研究提供可靠的依据。

1 试验方法

试验采用 1 mm 厚的 AZ31B 变形镁合金板(125 mm × 50 mm)和镀锌层为 60 g/m² 的镀锌钢板(125 mm × 50 mm), 直径为 1.6 mm 的 AZ61 镁合金焊丝, 其化学成分如表 1 ~ 表 3 所示。

表 1 AZ31B 镁合金板的化学成分(质量分数, %)

Table 1 Chemical compositions of AZ31B Mg alloy sheet

Al	Zn	Mn	Si	Mg
2.5 ~ 3.5	0.5 ~ 1.5	0.2 ~ 0.5	≤ 0.1	余量

表 2 镀锌钢板化学成分(质量分数, %)

Table 2 Chemical compositions of galvanized steel sheet

C	Mn	Si	P	S	Fe
0.12	0.39	≤ 0.3	0.03	0.025	余量

表 3 AZ61 镁合金焊丝化学成分(质量分数, %)

Table 3 Chemical compositions of AZ61 Mg Wire

Al	Zn	Mn	Cu	Mg
5.8 ~ 7.2	0.4 ~ 1.5	0.15 ~ 0.50	≤ 0.05	余量

试验采用的设备是 Fronius 公司生产的型号为 CMT3200 焊机和全自动焊接系统,焊接装置如图 1 所示. 焊前,先使用钻床在钢板上如图 1 所示位置上打孔,用砂纸和钢丝刷将镁合金试件表面的氧化膜去除,再用丙酮去除镁合金和镀锌钢板上的水渍和油污,将表面处理干净的试板组合成搭接接头(钢上镁下). 采用高纯氩气保护,其流量为 15 L/min. 根据预试验的结果,在一定范围内设计正交试验的各因素和水平,如表 4 所示. 结合焊点形貌、接头力学性能以及接头的显微组织特征,综合分析该焊接工艺的特性.

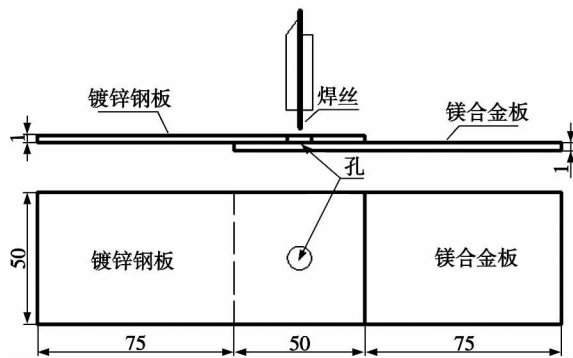


图 1 焊接装置示意图 (mm)

Fig. 1 Schematic diagram of welding device

表 4 正交试验的各因素和水平

Table 4 Orthogonal experiment level and factors

水平	因素 A 送丝速度 $v_f / (\text{m} \cdot \text{min}^{-1})$	因素 B 点焊时间 t / s	因素 C 钢板孔径 D / mm
1	12.5	0.6	6.0
2	13.0	0.8	8.0
3	13.5	1.0	9.0

2 试验结果和讨论

如正交试验表 5 所示,通过正交试验和极差、方差分析,由于试验的接头成形都十分良好,所以用接头所能承受的最大平均抗拉载荷作为评判标准,可得出试验的最佳工艺参数为送丝速度 13.5 m/min,点焊时间 1.0 s,钢板孔的直径 9 mm;工艺参数显著性顺序为镀锌钢板孔径大小、送丝速度、点焊时间.

2.1 焊点成形

图 2 为冷金属过渡 (cold metal transfer, CMT) 点焊时的焊点形貌,可以看出焊点表面成形良好,在焊接过程中镁合金焊丝熔化填充工艺孔,同时在镀锌钢板表面铺展,而其内在的机理需借助于接头组织

表 5 正交试验参数和结果

Table 5 Input parameters and output characteristics of orthogonal array

试验 编号	1 A	2 B	3 C	空白	平均载荷 F / kN
1	1	1	1	1	1.76
2	1	2	2	2	2.51
3	1	3	3	3	2.36
4	2	1	2	3	2.56
5	2	2	3	1	2.74
6	2	3	1	2	1.65
7	3	1	3	2	3.12
8	3	2	1	3	1.74
9	3	3	2	1	3.06

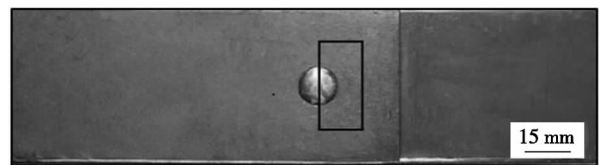


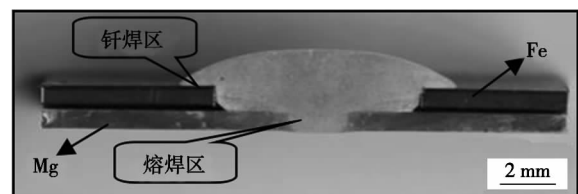
图 2 焊点形貌

Fig. 2 Welding appearance

进一步分析.

2.2 接头的宏观组织

图 3 为镁/钢异种金属 CMT 点熔钎焊的典型接头形貌,所取位置在图 2 中方框处. 可以发现当钢板孔径较大而热输入较小、时间较短时,形貌如图 3a 所示,此时接头的钎焊结合面和熔焊结合面都较小,会存在较大的间隙,而这些间隙可能会成为裂纹产生的源头. 当钢板孔径适中而热输入较大、时间较长时形貌如图 3b 所示,此时接头的钎焊结合面和熔焊结合面都较大,结合程度强. 通过大量试验



(a) 小参数下的焊接接头宏观组织



(b) 大参数下的焊接接头宏观组织

图 3 不同工艺参数下焊接接头的宏观组织

Fig. 3 Macrostructure of different process parameters

得到在送丝速度 13.0 ~ 13.5 m/min, 点焊时间 0.6 ~ 0.8 s, 钢板孔径 6 ~ 8 mm 时, 熔融的镁焊丝一方面能在镀锌钢板表面进行有效的铺展和润湿, 形成性能良好的钎焊结合面; 另一方面能和镁合金母材发生很好的熔合反应, 产生良好的熔焊接头, 最终形成具有优异力学性能的点熔钎焊接头。

2.3 接头的微观组织

图4为图3b中接头不同部位钎焊区界面和熔焊区熔合线附近的微观组织。可以看出, 在熔焊区熔融镁焊丝和镁合金板产生了很好的熔合, 其中图4a中A区为焊缝金属, 晶粒细小且分布均匀; B区为热影响区, 晶粒与A区中相比较明显粗大; C区为镁母材。钎焊区界面见图4b, 可以看出在结合面产生了12 μm 左右过渡区(图4b中1~4中间), 在1处有发白现象, 这是因为镁和钢硬度的差异过大, 镁较软导致在磨制抛光后界面处的镁和钢不在一个水平面上, 造成了在电镜成像时产生了边界效应的现象。表6为图4b中各点的扫描电镜能谱分析结果, 根据表6得出2处含有少量的Fe元素, 说明其发生了一定的扩散, 主要含有镁、锌以及少量的铝。根据镁-铝相图^[11]可知Al元素主要是和Mg元素产生脆性化合物 $\beta\text{-Mg}_2\text{Al}_3$, $\gamma\text{-Mg}_{17}\text{Al}_{12}$; 根据镁-锌相图^[12]可知当镁的原子含量达到66%时主要生成

$\alpha\text{-Mg}$ 和 MgZn 共晶相。而3处的成分和2处相似, 可知在界面过渡区主要是 $\alpha\text{-Mg}$ 和 MgZn 共晶相。4处和6处成分相似, 主要是 $\alpha\text{-Mg}$ 固溶体; 5处主要产生了 $\alpha\text{-Mg}$ 固溶体和镁铝锌化合物。

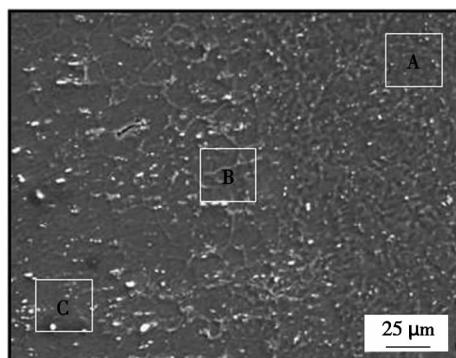
表6 SEM点分析成分(原子分数, %)

Table 6 Component of point analysis with SEM

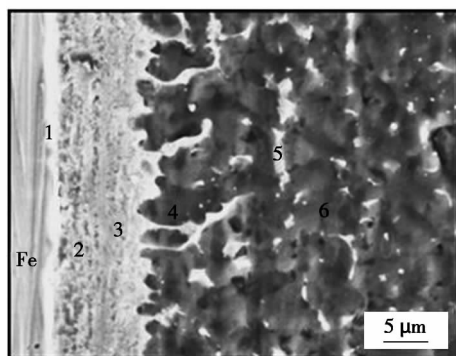
位置	Mg	Zn	Al	Fe
2	67.61	26.76	4.13	1.5
3	70.23	26.47	3.30	0
4	94.78	5.22	0	0
5	78.88	12.70	8.42	0
6	95.28	4.72	0	0

2.4 力学性能

采用标准试样, 考虑拉伸时试样两侧板不在一条中心线上, 所以在进行拉伸试验时在试样两侧使用相同厚度的垫片, 以保证试验结果的可靠性。拉伸试验的试验结果在前面正交试验表5中已给出, 可以发现当接头形式见图3a时, 其接头抗拉剪载荷在2 kN以下, 如表5中的1号试样。当接头形式见图3b时, 其接头抗拉剪载荷在3 kN左右, 如表5中的7号试样; 其断裂形貌见图5, 载荷一位移曲线如图6所示。由图5、图6可知, 当焊接参数较小时, 焊缝熔宽小见图3a, 拉伸试验时焊缝金属沿着镁板上表面直接被剪断, 所承载的载荷小; 当焊接参数较大时, 焊缝熔宽大见图3b, 拉伸时在焊点的热影响区发生断裂, 最终被撕裂。对两种断裂方式载荷一位



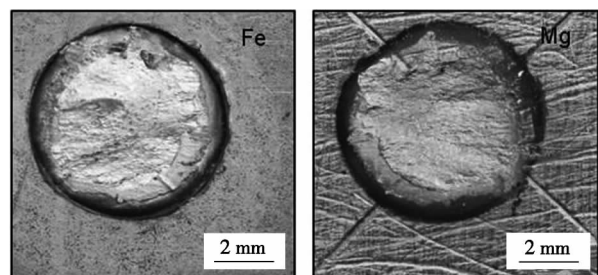
(a) 熔合区微观组织



(b) 钎焊界面微观组织

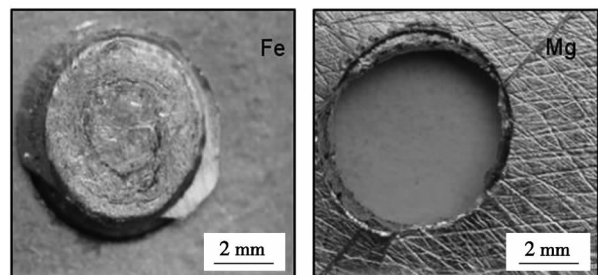
图4 接头不同位置的微观组织

Fig. 4 Microstructure of different positions of joint



(a) 1号试样钢侧剪切断裂

(b) 1号试样镁侧剪切断裂



(c) 7号试样钢侧撕裂形貌

(d) 7号试样镁侧撕裂形貌

图5 不同接头的断裂方式

Fig. 5 Fracture modes of different joints

移曲线进行比较发现剪断时,当达到最大载荷时,瞬时断裂;但是撕裂时,达到最大载荷后,载荷下降一部分后出现一个平台,经过一定位移后才会完全断裂.这一断裂方式经历了几个不同面的分阶段断裂.这种焊接接头在出现断裂后经过一段时间才会完全失效,在一定程度上保证了工件整体的安全性,特别是在汽车等交通工具上,可以更好的保障人身安全.同时也可以发现优化参数下镁/钢点焊的拉伸载荷可达 3.12 kN,远大于相同尺寸最佳镁/镁点焊试样的 1.8 kN 的拉剪载荷.

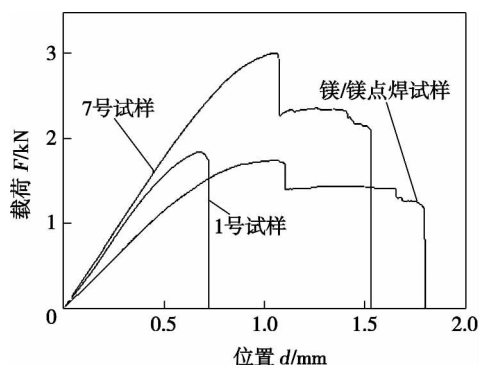


图 6 不同接头的载荷—位移曲线

Fig. 6 Load displacement curves of different joints

3 结 论

(1) 采用冷金属过渡点焊的方法可以实现镁/钢异种金属的有效连接,焊点成形和接头形貌良好.

(2) 在一定范围内载荷随着热输入和钢板孔径的增大而增大,当送丝速度 13.5 m/min,点焊时间 0.6 s,钢板孔径 9 mm 时,接头达到最大载荷 3.12 kN.

(3) 焊接接头为典型的点熔钎焊接头,分别由钎焊结合区和熔焊结合区组成,在钎焊区镁/钢界面形成 12 μm 厚的 $\alpha\text{-Mg}$ 和 MgZn 共晶相的结合层.

(4) 在一定范围内当焊接参数较小时,接头的断裂方式为剪切断裂,性能较差;当焊接参数较大时,接头断裂方式为撕裂,性能良好.

参考文献:

[1] 陈 军. 镁合金在汽车工业中应用与分析[J]. 材料研究与

应用,2010,4(6): 81-84.

Chen Jun. Application analysis of magnesium alloy in automotive industry[J]. Materials Research and Application, 2010, 4(6): 81-84.

[2] Chen Minghua, Li Chenbin, Yuan Shengtao, et al. High-speed butt welding of magnesium alloy using pulsed laser-arc hybrid heat source[J]. China Welding, 2012, 21(1): 1-7.

[3] 顾钰熹. 特种工程材料焊接[M]. 沈阳: 辽宁科学技术出版社, 1998.

[4] 李亚江,王 娟,刘 鹏. 异种难焊材料的焊接及应用[M]. 北京: 化学工业出版社, 2003.

[5] Pierre D, Viala J C, Peronnet M, et al. Interface reactions between mild steel and liquid Mg-Mn alloys[J]. Material Science and Engineer A, 2003, 34(9): 256-264.

[6] Chen Y C, Nakata K. Effect of tool geometry on microstructure and mechanical properties of friction stir lap welded magnesium alloy and steel[J]. Materials and Design, 2009, 30(9): 3913-3919.

[7] 黄勇兵,李建萍,黄春平,等. 镁和钢搅拌摩擦焊接头组织分析[J]. 焊接学报, 2013, 34(5): 67-70.

Huang Yongbing, Li Jianping, Huang Chunping, et al. Micro-structure of friction stir welded joint of magnesium and steel[J]. Transactions of the China Welding Institution, 2013, 34(5): 67-70.

[8] Qi Xiaodong, Song Gang. Interfacial structure of the joints between magnesium alloy and mild steel with nickel as interlayer by hybrid laser-TIG welding[J]. Materials and Design, 2010, 31(1): 605-609.

[9] 单 闯,宋 刚,刘黎明. 激光-TIG 复合热源焊接参数对镁/钢异种材料焊接接头的影响[J]. 焊接学报, 2008, 29(6): 57-60.

Shan Chuang, Song Gang, Liu Liming. Effect of laser-TIG hybrid welding parameters on joint of Mg to steel[J]. Transactions of the China Welding Institution, 2008, 29(6): 57-60.

[10] 苗玉刚,韩端峰,姚竞争. 镁/钢异种金属激光深熔钎焊工艺特性[J]. 焊接学报, 2011, 32(1): 45-48.

Miao Yugang, Han Duanfeng, Yao Jingzheng. Welding characteristic of laser welding-brazed Mg/steel dissimilar alloys[J]. Transactions of the China Welding Institution, 2011, 32(1): 45-48.

[11] Wahba M, Katayama S. Laser welding of AZ31B magnesium alloy to Zn-coated steel[J]. Materials and Design, 2012, 35: 701-706.

[12] 郭青蔚,王桂生,郭庚辰. 常用有色金属二元合金相图[M]. 北京: 化学工业出版社, 2010.

作者简介: 许庆伟,男,1986 年出生,硕士研究生. 主要从事异种金属的焊接性研究. Email: xuqingwei1986@126.com

通讯作者: 曹 睿,女,教授,硕士研究生导师. Email: caorui@lut.cn

Abstract: The brazing of C/C composite and GH99 nickel base superalloy was successfully performed using BNi2 + TiH₂ brazing powder. The interfacial microstructure and mechanical properties of the brazed joints were investigated. The results show that , the typical microstructure of the joint is: C/C composite/Cr₃C₂ + MC + Ni(s s) /MC + Ni(s s) /Ni₃Si + Ni(s s) /Cr₃C₂ + MC + Ni(s s) /GH99. With the increasing of content of TiH₂ , the dissolution of C/C substrate was enhanced , dispersed MC carbide particles formed in braze seam , and the modulus mismatch between C/C and filler alloy , the mechanical properties of the brazed joints were improved consequently. When using braze powder with 3% TiH₂ addition , the maximum shear strength of the brazed joints were obtained , which were 40 MPa at room temperature , 19 MPa at 800 °C and 10 MPa at 1 000 °C. Comparing with brazed joints using BNi2 filler alloy , BNi2 + TiH₂ joints possess higher strength , and the high-temperature properties of the joints can be guaranteed.

Key words: C/C composite; GH99 superalloy; BNi2 + TiH₂ braze powder; interfacial microstructure; mechanical properties

Microstructure and mechanical properties of impact pressure transient liquid phase bonded Mg/Al

LIU Meng'en^{1,2} , SHENG Guangmin¹ (1. College of Material Science and Engineering , Chongqing University , Chongqing 400044 , China; 2. Chongqing Industry Polytechnic College , Faculty of Vehicle Engineering , Chongqing 401120 , China) . pp 39 – 42

Abstract: Diffusion bonding of magnesium alloy AZ31 and Al5083 was undertaken under an impact pressure in vacuum. The microstructural features , mechanical properties of the joints were investigated by scanning electron microscopy (SEM) , energy Dispersive spectrometer(EDS) , microhardness tester and x-ray diffractometer. The results show that the joints are formed four layers , such as magnesium alloy matrix , metallurgical reaction layer , diffusion layer and aluminum alloy matrix. There are the intermetallic compounds Mg₂Al₃ , MgAl , Al_{0.56}Mg_{0.44} , and the highest hardness is 3 300 MPa in the joint zone. The tensile test results show that the tensile strength of the joint increases at first then decreases , and an optimized bonding strength of up to 46MPa. The tensile fracture is mixture of quasi cleavage and dimple. There exists prevailing information asymmetry in the mg side and al side.

Key words: impact pressure; diffusion bonding; microstructure; tensile strength

Process characteristics of cold metal transfer spot welding for automotive dissimilar metals between magnesium and steel

XU Qingwei¹ , CAO Rui¹ , CHEN Jianhong¹ , WANG Peichung² (1. State Key Laboratory of Advanced processing and Recycling of Non-ferrous Metals , Lanzhou University of Technology , Lanzhou 730050 , China; 2. GM R&D Center , Warren MI 48090 , USA) . pp 43 – 46

Abstract: The magnesium alloy AZ31B sheet and galvanized steel sheet were lapped by cold metal transfer spot welding. Using orthogonal test method to optimize process parameters and at the same time , by means of optical microscope , scanning

electron microscopy and universal tensile testing machine , the microstructure and mechanical properties of welding joint were studied. The results show that satisfied weld appearance and properties can be obtained. The important sequence of process parameters are followed , size of hole on the galvanized steel sheet , wire feed speed , spot welding time. The joints are typical spot welding-brazing joint , which are composed by the brazing zone and the welding zone. The tensile shear load of joint can reach 3. 12 kN , which is larger than that of Mg-Mg spot welding joints. The shear fracture and tear fracture dominate the fracture mode of the joint.

Key words: cold metal transfer spot welding; dissimilar metals; process characteristics; orthogonal test

Y-groove cracking test on the welding crack resistance of the NM400 steel

WANG Lipeng , ZHOU Guangtao (College of mechanical engineering and automation , Huaqiao University , Xiamen 361021 , China) . pp 47 – 50

Abstract: Y-groove cracking test was conducted to study the welding crack resistance of NM400 steel. Assessment of welding crack resistance of steel NM400 consists of the surface crack rate , section crack rate and root crack rate , and the effects of preheating on the crack resistance of steel NM400 has been analyzed. Thermal elastic-plastic finite element method was applied to carry out a finite numerical simulation of welding process for samples used in Y-groove cracking test and transverse welding residual stress distribution and peak position were obtained. The results indicated that the root crack rate of the steel NM400 at room temperature reached a high value , and it could be decreased to zero when preheating at 150 °C. Therefore , preheating before welding can improve the welding crack resistance of steel NM400. Otherwise , stress concentration occurred at the root of the Y-groove. Local transverse residual stress which was larger than the yield strength of materials is mechanical factors causing cracks.

Key words: welding crack resistance; finite element simulation; preheating

Property of repair welding joint of A7N01 aluminium alloy

YAN Zhongjie¹ , CHEN Shuxiang² , SHANG Zhe³ , LIU Xuesong¹ , FANG Hongyuan¹ (1. State Key Laboratory of Advanced Welding and Joining , Harbin Institute of Technology , Harbin 150001 , China; 2. CSR Sifang Locomotive and Rolling Stock. Co. , LTD , Qingdao 26111 , China; 3. Beijing Aerospace Xinfeng Mechanical Equipment. Co. , LTD , Beijing 100070 , China) . pp 51 – 54

Abstract: The welding joint and repair welding joint of A7N01 aluminium alloy are analyzed in this paper , the mechanical properties of the welding joint before and after repair welding were studied by welding residual stress measurement , tensile test , micro-hardness test , metallographic observation and fracture toughness test , respectively. Based on the fracture toughness theory , the critical crack length of the structure before and after repair welding is calculated. With the initial crack length determined by metallographic observation , the residual fatigue life before and after repair welding is calculated using Paris for-